A Unified Approach to Solving the Harmonic Elimination Equations in Multilevel Converters

John N. Chiasson, *Senior Member, IEEE*, Leon M. Tolbert, *Senior Member, IEEE*, Keith J. McKenzie, *Student Member, IEEE*, and Zhong Du, *Student Member, IEEE*

***Abstract*—A method is presented to compute the switching angles in a multilevel converter so as to produce the required fundamental voltage while at the same time not generate higher order harmonics. Using a staircase fundamental switching scheme, previous work has shown that this is possible only for specific ranges of the modulation index. Here it is shown that, by considering all possible switching schemes, one can extend the lower range of modulation indices for which such switching angles exist. A unified approach is presented to solve the harmonic elimination equations for all of the various switching schemes. In particular, it is shown that all such schemes require solving the *same* set of equations where each scheme is distinguished by the location of the roots of the harmonic elimination equations. In contrast to iterative numerical techniques, the approach here produces all possible solutions.**

***Index Terms*—Harmonic elimination, multilevel inverter, symmetric polynomials.**

I. Introduction

THE GENERAL function of the multilevel inverter is to synthesize a desired ac voltage from several levels of dc voltages. For this reason, multilevel inverters are ideal for connecting either in series or in parallel an ac grid with distributed energy resources such as photovoltaics (solar cells), fuel cells or with energy storage devices such as capacitors or batteries [1]. Additional applications of multilevel converters include such uses as medium voltage adjustable speed motor drives, static var compensation, dynamic voltage restoration, harmonic filtering, or for a high voltage dc back-to-back intertie [2]. Transformerless multilevel inverters are uniquely suited for this application because of the high VA ratings possible with these inverters [3]. It is the unique structure of the multilevel voltage source inverter which allows it to reach high voltages with low harmonics without the use of transformers or series-connected, synchronized-switching devices.

A fundamental issue in the control of a multilevel converter is to determine the switching angles (times) so that the converter produces the required fundamental voltage and does not generate specific lower order dominant harmonics. Using a staircase scheme as illustrated in Fig. 3(a), it has been shown in [4], [5] that this is possible only for modulation indices m_a between approximately 0.38 and 0.84 (see Fig. 2 where $m_a = m/s$ and $s = 3$ is the number of separate dc sources). However, there are other possible switching schemes which may work over different ranges of the modulation index or, even work for $0.38 \leq m_a \leq 0.84$ and provide solutions with a lower total harmonic distortion (THD) than the staircase scheme. For example, in [6] the authors considered the output waveform shown in Fig. 3(f) which they referred to as a "virtual stage" waveform. Here, the objective is to systematically consider every possible switching scheme (output waveform) that switches at nearly the fundamental frequency. A general unified approach is presented to solving the harmonic elimination equations for *all* solutions of *all* possible switching schemes. That is, the approach provides both the scheme and the particular set of switching angles that produce the lowest THD for any given modulation index. In contrast to PWM techniques (e.g., see [7]), the switching schemes proposed here are only slightly above the fundamental frequency resulting in low switching losses.

The unified approach demonstrated here is accomplished by first transforming the nonlinear transcendental harmonic elimination equations for all possible switching schemes into a *single set* of *symmetric* polynomial equations. Then it is shown that a particular switching scheme is simply characterized by the location of the roots of these polynomial equations. The complete set of solutions to the equations are found using the method of resultants from elimination theory [8]. In contrast to iterative numerical techniques (e.g., see [6] and [9]), the approach here produces all possible solutions. Experimental results using the approach are also presented and indicate close agreement with predicted results.

II. Cascaded H-Bridges

The cascade multilevel inverter consists of a series of H-bridge (single-phase full-bridge) inverter units. As stated above, the general function of the multilevel inverter is to synthesize a desired voltage from several separate dc sources (SDCSs) such as solar cells, fuel cells, ultracapacitors, etc. Fig. 1 shows a single-phase structure of a cascade inverter with SDCSs [3]. Each SDCS is connected to a single-phase full-bridge inverter and can generate three different voltage outputs, $+V_{dc}$, 0 and $-V_{dc}$. This is accomplished by connecting the dc source to the ac output side by using different combinations of the four switches, S_1, S_2, S_3 and S_4. The ac output of each level's full-bridge inverter is connected in series such that the synthesized voltage waveform is the sum of all of the individual inverter outputs. The number of output phase (line-neutral) voltage levels in a cascade mulitilevel inverter is then $2s + 1$, where s is the number of dc sources. An example

Manuscript received June 25, 2003; revised September 5, 2003. This work was supported in part by the National Science Foundation through Grant NSF ECS-0093884 and the Oak Ridge National Laboratory under UT/Battelle Contract 4000007596. Recommended by Associate Editor J. R. Rodriguez.

The authors are with the Electrical and Computer Engineering Department, The University of Tennessee, Knoxville, TN 37996-2100 USA (e-mail: chiasson@utk.edu; tolbert@utk.edu; kmc18@utk.edu; zdu1@utk.edu).

Digital Object Identifier 10.1109/TPEL.2003.823198

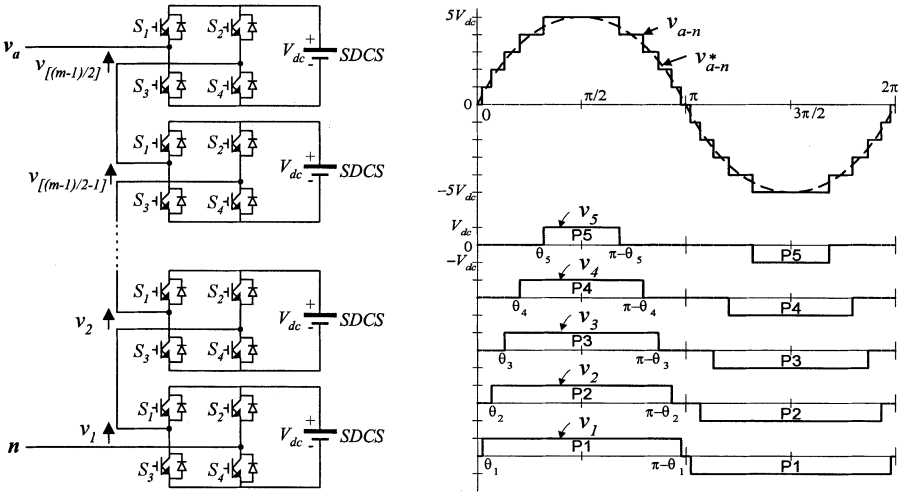

(a) (b)

Fig. 1. (a) Schematic layout of a multilevel inverter. (b) Staircase waveform produced by a 5 SDCS multilevel inverter.

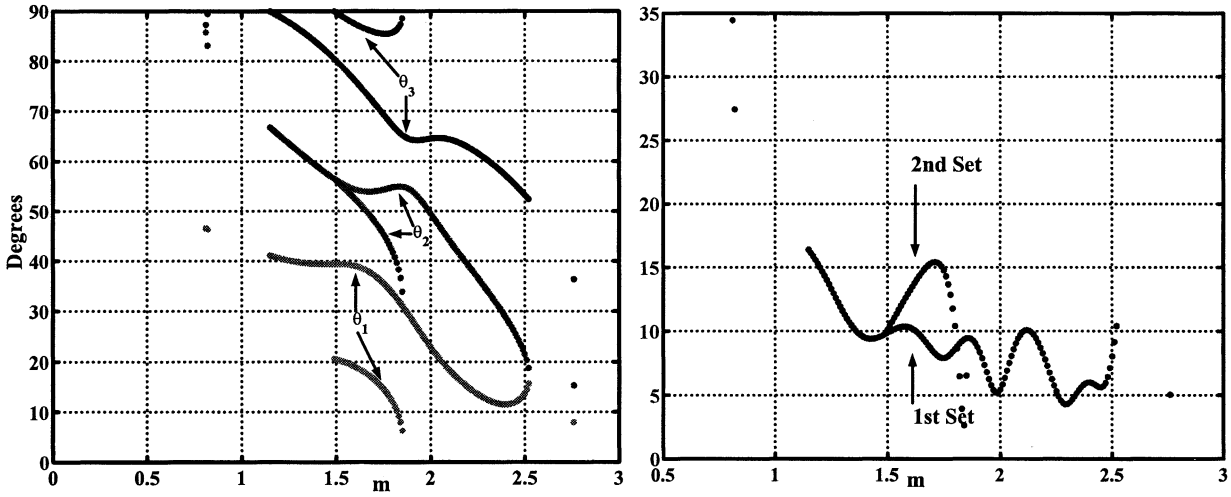

(a) (b)

Fig. 2. (a) Switching angles θ_1, θ_2, θ_3 versus m for the staircase scheme of Fig. 3(a). (b) The THD versus m for each solution set.

phase voltage waveform for an 11-level cascaded multilevel inverter with five SDSCs ($s = 5$) is shown in Fig. 1. The output phase voltage is given by $v_{an} = v_{a1} + v_{a2} + v_{a3} + v_{a4} + v_{a5}$.

Each of the active devices of the H-bridges switch only at the fundamental frequency, and consequently this is referred to as the fundamental switching scheme. Also, each H-bridge unit generates a quasisquare waveform by phase-shifting its positive and negative phase legs' switching timings. Further, each switching device always conducts for 180° or 1/2 cycle regardless of the pulse width of the quasisquare wave so that this switching method results in equalizing the current stress in each active device.

Using the staircase scheme of Fig. 1 [see also Fig. 3(a)], it has been shown in [4] that one can obtain the fundamental while eliminating specified lower order harmonics only for certain ranges of the modulation index. For example, the left side of Fig. 2 is a plot of the switching solution angles in the case of three dc sources where the fundamental is achieved while the fifth and seventh harmonics are eliminated. Here the parameter m is related to the modulation index by $m = sm_a$ where s is the number of dc sources ($s = 3$ in Fig. 2). Note that for m in the interval [1.15,2.52] there is a solution (with two different sets of solutions in the subinterval [1.49,1.85]). On the other hand, for $m \in [0, 0.8]$, $m \in [0.83, 1.14]$ and $m \in [2.53, 2.76]$ there are *no* solutions. As Fig. 2 illustrates, there is a significant range of the modulation index for which there is no solution.

The objective here is to show how the range of values of the modulation index $m_a = m/s$ can be extended for which the fundamental is still achieved and the fifth and seventh harmonics are also eliminated. This is done in the case at hand by having one more switching per cycle than the staircase scheme. At very low modulation indices, one would surmise that only one of the dc sources would be used with multiple switchings on that source. This is indeed the case and is simply the unipolar programmed PWM switching scheme of Patel and Hoft [10], [11] [see Fig. 3(b)]. At slightly higher modulation indices one would

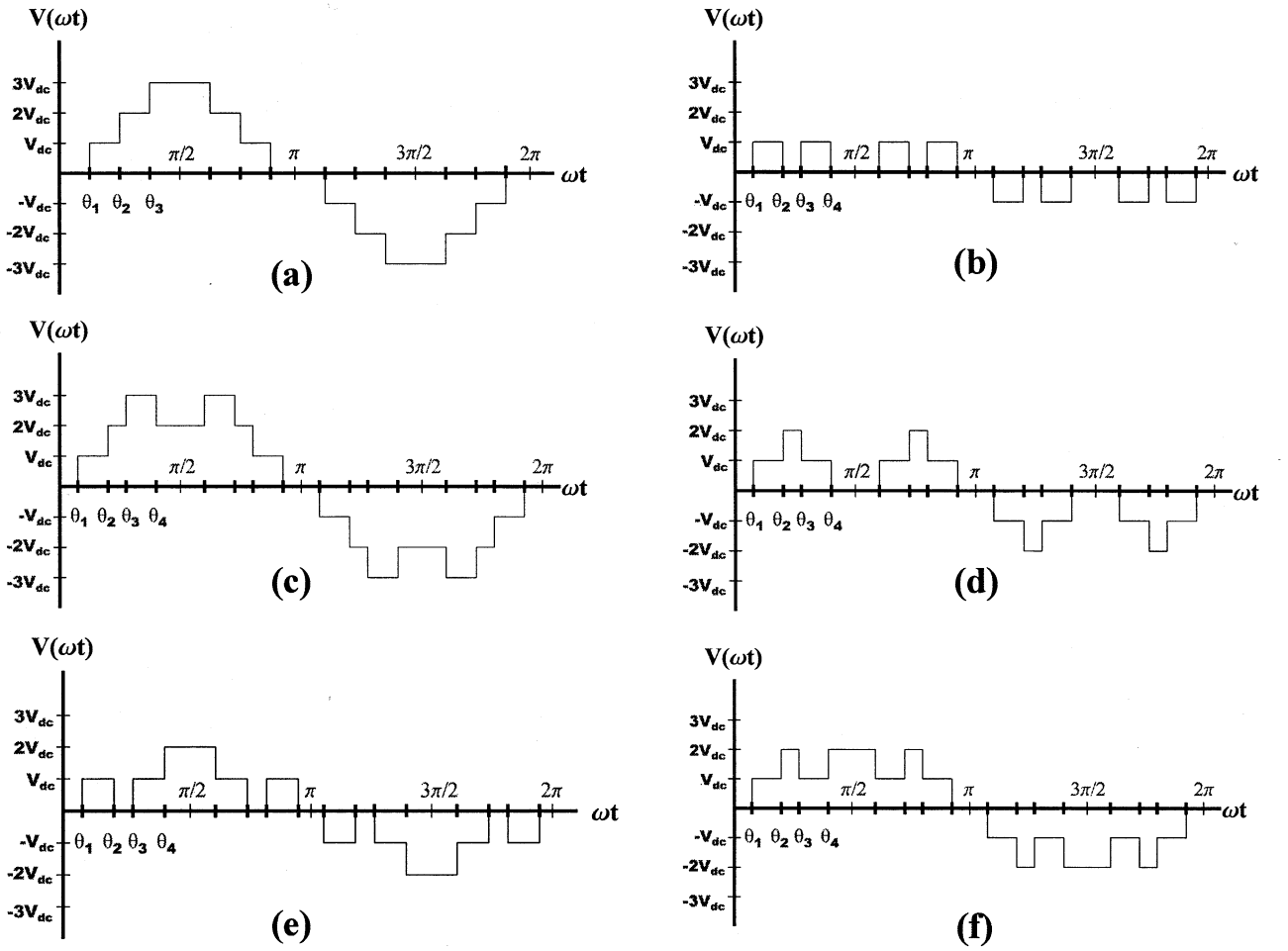

Fig. 3. Possible switching schemes for a 3 dc source multilevel converter.

surmise that two dc sources would be used with a scheme such as in [6] [see Fig. 3(f)] or a combination of the unipolar scheme and that of two dc source multilevel scheme as in Fig. 3(e). In the following, it is shown how the transcendental equations that characterize the harmonic content for each of these switching schemes can be solved to find *all* solutions that eliminate the fifth and seventh harmonics while achieving the fundamental.

III. Mathematical Model of Switching

The scheme shown in Fig. 1 is not the only possible scheme to eliminate harmonics in a multilevel converter. To illustrate, let $s = 3$ and limit the number of switchings to four per quarter cycle. In this case, the possible switching schemes are drawn in Fig. 3(a)–(f). Note that Fig. 3(a) is a special case of Fig. 3(c) with $\theta_4 = \pi/2$. The objective is to consider the possibility that the schemes shown in Fig. 3(b)–(f) can provide a solution at modulation indices where the staircase scheme of Fig. 3(a) is unable to do so or provide a solution with a lower THD. These schemes use four switching angles in contrast to the three switching angles used by the staircase switching scheme of Fig. 3(a). Consequently, their switches turn on and off at an overall frequency just above the fundamental frequency.

To proceed, note that each of the waveforms of Fig. 3(b)–(f) have a Fourier series expansion of the form

$$V(\omega t) = \frac{4V_{dc}}{\pi}\sin(n\omega t) \times \sum_{n=1,3,5,\ldots}^{\infty} \frac{1}{n}\left(\ell_1\cos(n\theta_1) + \ell_2\cos(n\theta_2) + \ell_3\cos(n\theta_3) + \ell_4\cos(n\theta_4)\right) \quad (1)$$

where $0 \le \theta_1 \le \theta_2 \le \theta_3 \le \theta_4 \le \pi/2$ and $\ell_i = \pm 1$ depending on the switching scheme as shown in the table given in (2), shown at the bottom of the next page. For each of these schemes, the Fourier series is summed over only the *odd* harmonics, and as $\cos(n(\pi - \theta_i)) = -\cos(n\theta_i)$ for n odd, (1) may be rewritten in the form

$$V(\omega t) = \frac{4V_{dc}}{\pi}\sin(n\omega t) \times \sum_{n=1,3,5,\ldots}^{\infty} \frac{1}{n}\left(\cos(n\theta_1') + \cos(n\theta_2') + \cos(n\theta_3') + \cos(n\theta_4')\right)$$

where $\theta_i' = \theta_i$ if $\ell_i = 1$ and $\theta_i' = \pi - \theta_i$ if $\ell_i = -1$. In terms of the angles θ_i', the conditions $\theta_1 \le \theta_2 \le \theta_3 \le \theta_4$ become those in the right-most column of the table in (2). Again, the

desire here is to use these switching schemes to achieve the fundamental voltage and eliminate the fifth and seventh harmonics for those values of the modulation index m_a for which solutions did not exist (see Fig. 2) for the switching scheme of Fig. 3(a). That is, choose the switching angles θ_1', θ_2', θ_3', θ_4' to satisfy

$$\begin{aligned}\cos(\theta_1')+\cos(\theta_2')+\cos(\theta_3')+\cos(\theta_4') &= m\\ \cos(5\theta_1')+\cos(5\theta_2')+\cos(5\theta_3')+\cos(5\theta_4') &= 0\\ \cos(7\theta_1')+\cos(7\theta_2')+\cos(7\theta_3')+\cos(7\theta_4') &= 0\end{aligned} \quad (3)$$

and the inequalities (2). Here $m \triangleq V_1/(4V_{dc}/\pi)$ and the modulation index is given by $m_a \triangleq m/s$ where s (= 3 here) is the number of dc sources. This is a system of three transcendental equations in the four unknowns θ_1', θ_2', θ_3', θ_4'. In order to get a fourth constraint, consider the possibility of also eliminating the 11th harmonic using this extra switching. In other words, one appends the condition

$$\cos(11\theta_1')+\cos(11\theta_2')+\cos(11\theta_3')+\cos(11\theta_4')=0 \quad (4)$$

to the conditions (3). The fundamental question is "When does the set of transcendental equations (3) and (4) have a solution?" The correct solution to the conditions (3) and (4) would mean that the output voltage would not contain the fifth, seventh and 11th order harmonic components. One approach to solving the set of nonlinear transcendental equations (3), (4) is to use an iterative method such as the Newton–Raphson method [2], [12]. In contrast to iterative methods, the approach here is based on solving polynomial equations using the theory of resultants which produces *all* possible solutions [8], [13]. The first step requires transforming the transcendental equations (3) and (4) into *polynomial* equations using the change of variables

$$\begin{aligned}x_1 &= \cos(\theta_1'), \quad x_2 = \cos(\theta_2'),\\ x_3 &= \cos(\theta_3'), \quad x_4 = \cos(\theta_4')\end{aligned}$$

and the trigonometric identities

$$\begin{aligned}\cos(5\theta) &= 5\cos(\theta)-20\cos^3(\theta)+16\cos^5(\theta)\\ \cos(7\theta) &= -7\cos(\theta)+56\cos^3(\theta)-112\cos^5(\theta)+64\cos^7(\theta)\\ \cos(11\theta) &= -11\cos(\theta)+220\cos^3(\theta)-1232\cos^5(\theta)\\ &\quad +2816\cos^7(\theta)-2816\cos^9(\theta)+1024\cos^{11}(\theta).\end{aligned}$$

The (3) and (4) then become the equivalent conditions

$$\begin{aligned}p_1(x) &\triangleq x_1+x_2+x_3+x_4-m=0\\ p_5(x) &\triangleq \sum_{i=1}^{4}\left(5x_i-20x_i^3+16x_i^5\right)=0\\ p_7(x) &\triangleq \sum_{i=1}^{4}\left(-7x_i+56x_i^3-112x_i^5+64x_i^7\right)=0\\ p_{11}(x) &\triangleq \sum_{i=1}^{4}\left(-11x_i+220x_i^3-1232x_i^5+2816x_i^7\right.\\ &\quad \left.-2816x_i^9+1024x_i^{11}\right)\end{aligned} \quad (5)$$

where $x \triangleq (x_1, x_2, x_3, x_4)$, and the angle conditions become

Scheme	Inequality Conditions
Fig. 3(b)	$0 \le -x_4 \le x_3 \le -x_2 \le x_1 \le 1$
Fig. 3(c)	$0 \le -x_4 \le x_3 \le x_2 \le x_1 \le 1$
Fig. 3(d)	$0 \le -x_4 \le -x_3 \le x_2 \le x_1 \le 1$
Fig. 3(e)	$0 \le x_4 \le x_3 \le -x_2 \le x_1 \le 1$
Fig. 3(f)	$0 \le x_4 \le -x_3 \le x_2 \le x_1 \le 1$

. (6)

System (5) is a set of four polynomial equations in the four unknowns x_1, x_2, x_3, x_4. In the next section, a systematic method is presented to solve these equations for all of their possible solutions. Further, for each x_i with $-1 \le x_i \le 1$, there is a *unique* solution to $x_i = \cos(\theta_i')$ for the θ_i' with $0 \le \theta_i' \le \pi$. This then implies a unique solution for the switching angle θ_i in the interval $0 \le \theta_i \le \pi/2$ via $\theta_i = \theta_i'$ if $0 \le \theta_i' \le \pi/2$ and $\theta_i = \pi - \theta_i'$ if $\pi/2 \le \theta_i' \le \pi$.

Polynomial systems were also considered to compute the solutions of the harmonic elimination equations by iterative numerical methods in [14]. In contrast, here it is shown how all possible solutions of (5) can be found.

IV. Solving Polynomial Equations

The first equation of (5) can be solved as $x_4 = m - (x_1 + x_2 + x_3)$ to eliminate x_4 from the remaining three equations obtaining

$$\begin{aligned}q_5(x_1,x_2,x_3) &\triangleq p_5(x_1,x_2,x_3,m-x_1-x_2-x_3)\\ q_7(x_1,x_2,x_3) &\triangleq p_7(x_1,x_2,x_3,m-x_1-x_2-x_3)\\ q_{11}(x_1,x_2,x_3) &\triangleq p_{11}(x_1,x_2,x_3,m-x_1-x_2-x_3).\end{aligned} \quad (7)$$

Scheme	$\boldsymbol{\ell} = (\ell_1, \ell_2, \ell_3, \ell_4)$	Inequality Condition
Fig. 3 (b)	$(+1,-1,+1,-1)$	$0 \le \theta_1' \le \pi - \theta_2' \le \theta_3' \le \pi - \theta_4' \le \frac{\pi}{2}$
Fig. 3 (c)	$(+1,+1,+1,-1)$	$0 \le \theta_1' \le \theta_2' \le \theta_3' \le \pi - \theta_4' \le \frac{\pi}{2}$
Fig. 3 (d)	$(+1,+1,-1,-1)$	$0 \le \theta_1' \le \theta_2' \le \pi - \theta_3' \le \pi - \theta_4' \le \frac{\pi}{2}$
Fig. 3 (e)	$(+1,-1,+1,+1)$	$0 \le \theta_1' \le \pi - \theta_2' \le \theta_3' \le \theta_4' \le \frac{\pi}{2}$
Fig. 3 (f)	$(+1,+1,-1,+1)$	$0 \le \theta_1' \le \theta_2' \le \pi - \theta_3' \le \theta_4' \le \frac{\pi}{2}$

(2)

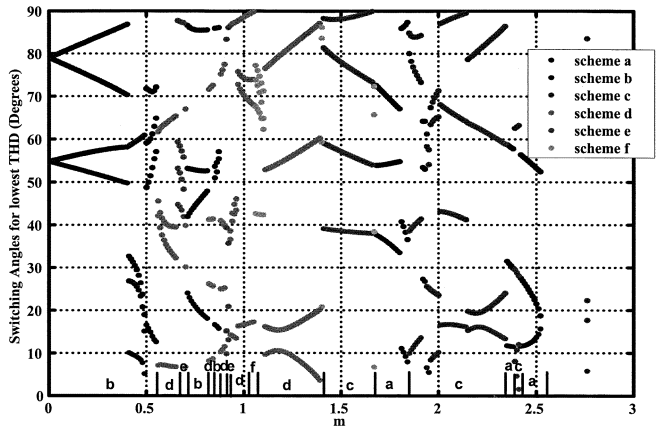

Fig. 4. Switching angles versus m which give the smallest THD.

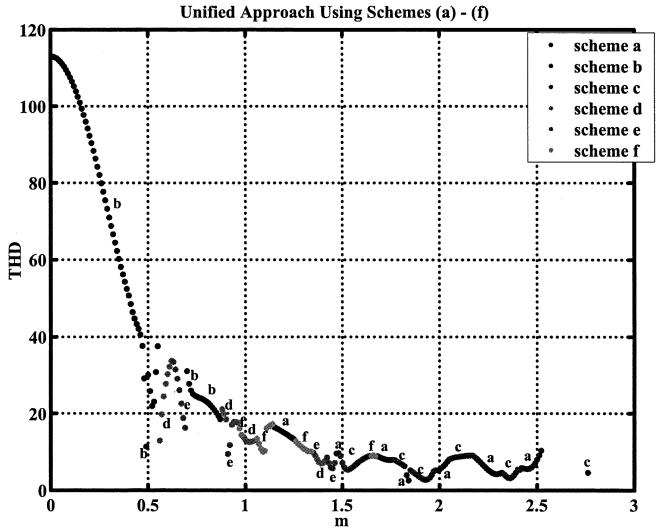

Fig. 5. THD versus m for the switching schemes and angles that give the smallest THD.

However, one is still left with three polynomial equations in the three unknowns (x_1, x_2, x_3). The pertinent question is then, "Given two polynomial equations $a(x_1,x_2,x_3)=0$ and $b(x_1,x_2,x_3)=0$, how does one solve them simultaneously to eliminate (say) x_3?" A systematic procedure to do this is known as *elimination theory* and uses the notion of *resultants* [8], [13]. Briefly, one considers $a(x_1,x_2,x_3)$ and $b(x_1,x_2,x_3)$ as polynomials in x_3 whose coefficients are polynomials in (x_1, x_2). Then, for example, letting $a(x_1,x_2,x_3)$ and $b(x_1,x_2,x_3)$ have degrees 3 and 2, respectively in x_3, they may be written in the form

$$\begin{aligned} a(x_1,x_2,x_3) &= a_3(x_1,x_2)x_3^3 + a_2(x_1,x_2)x_3^2 \\ &\quad + a_1(x_1,x_2)x_3 + a_0(x_1,x_2) \\ b(x_1,x_2,x_3) &= b_2(x_1,x_2)x_3^2 + b_1(x_1,x_2)x_3 + b_0(x_1,x_2). \end{aligned}$$

The $n \times n$ *Sylvester* matrix $S_{a,b}$, where $n = \deg_{x_3}\{a(x)\} + \deg_{x_3}\{b(x)\} = 3+2=5$, is defined by the equation shown at the bottom of the next page. The *resultant polynomial* $r(x_1,x_2)$ is defined by

$$\begin{aligned} r(x_1,x_2) &= \operatorname{Res}(a(x_1,x_2,x_3), b(x_1,x_2,x_3), x_3) \\ &\triangleq \det S_{a,b}(x_1,x_2) \end{aligned} \tag{8}$$

TABLE I
SCHEME THAT RESULTS IN THE LOWEST THD FOR A GIVEN INTERVAL OF m

m	$0-0.55$	$0.56-0.62$	$0.63-0.69$	$0.7-0.87$	$0.88-0.9$	$0.91-0.92$
scheme	b	d	e	b	d	e
m	$0.93-0.96$	$0.97-0.98$	$0.99-1.05$	$1.06-1.14$	$1.15-1.25$	$1.26-1.34$
scheme	d	f	d	f	a	f
m	$1.36-1.41$	$1.42-1.46$	$1.47-1.48$	$1.49-1.64$	$1.65-1.67$	$1.68-1.76$
scheme	d	e	a	c	f	a
m	$1.77-1.82$	$1.83-1.84$	$1.85-1.97$	$1.98-2.05$	$2.06-2.18$	$2.19-2.32$
scheme	c	a	c	a	c	a
m	$2.33-2.41$	$2.42-2.52$	$2.76-2.76$			
scheme	c	a	c			

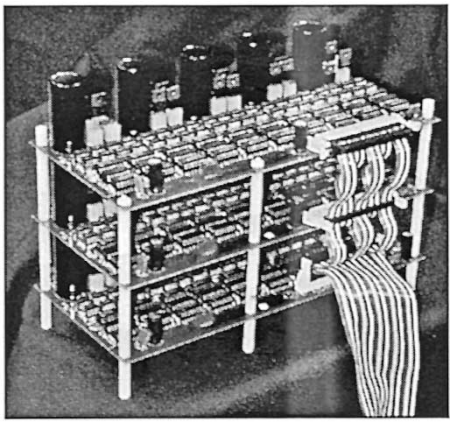

Fig. 6. Gate driver boards and MOSFETs for the mulitlevel inverter.

TABLE II
SDCS VOLTAGE VALUES

	Phase a	Phase b	Phase c
DC source 1	38.66 V	38.70 V	38.58 V
DC source 2	38.66 V	38.64 V	38.67 V
DC source 3	38.54 V	38.40 V	38.56 V

and is the result of solving $a(x_1,x_2,x_3)=0$ and $b(x_1,x_2,x_3)=0$ simultaneously for (x_1, x_2), i.e., eliminating x_3. See the Appendix for more details on resultants.

To proceed, one then eliminates x_1 from the system (7) by computing

$$\begin{aligned} r_{q_5,q_7}(x_2,x_3) &\triangleq \operatorname{Res}(q_5(x_1,x_2,x_3), q_7(x_1,x_2,x_3), x_1) \\ r_{q_5,q_{11}}(x_2,x_3) &\triangleq \operatorname{Res}(q_5(x_1,x_2,x_3), q_{11}(x_1,x_2,x_3), x_1) \end{aligned}$$

and finally, eliminating x_3 from $r_{q_5,q_7}(x_2,x_3)$ and $r_{q_5,q_{11}}(x_2,x_3)$ by computing

$$r(x_2) \triangleq \operatorname{Res}(r_{q_5,q_7}(x_2,x_3), r_{q_5,q_{11}}(x_2,x_3), x_3)$$

results in a single polynomial in the single variable x_2. For each m, one solves $r(x_2)=0$ for the roots $\{x_{2i}\}$. Each root x_{2i} is then used to solve $r_{q_5,q_7}(x_{2i},x_3)=0$ for the roots $\{x_{3j_i}\}$. Each pair (x_{2i},x_{3j_i}) is then used to solve $q_5(x_1,x_{2i},x_{3j_i})=0$ to obtain the roots $x_{1k_{i,j}}$. The set of 4-tuples $\{x|(x_1,x_2,x_3,x_4)=$

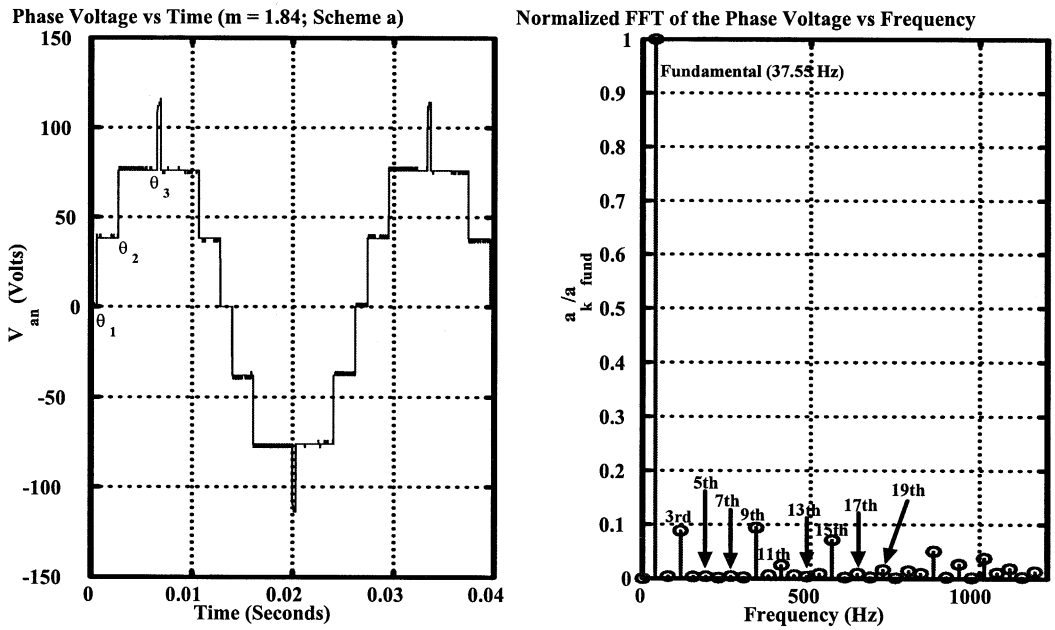

(a) (b)

Fig. 7. (a) Scheme *a* voltage waveform for $m = 1.84$. (b) Corresponding FFT.

$(x_{1k_{i,j}}, x_{2i}, x_{3j_i}, m - x_{1k_{i,j}} - x_{2i} - x_{3j_i})$ for some $i, j, k\}$ are then the only possible solutions to (5).

V. Computational Results

Using the above techniques, the switching angles for each switching scheme versus the parameter m (modulation index is $m_a = m/s$) were computed. For each value of m, it is possible that more than one waveform switching scheme of Fig. 3 will result in eliminating the fifth, seventh, and 11th harmonics. Further, each such waveform scheme may have also more than one set of angles for which the fifth, seventh, and 11th harmonics are eliminated. The scheme and set of switching angles that produced the smallest THD were chosen for each value of m and are plotted in Fig. 4. The corresponding harmonic distortion in percent defined by

$$THD \triangleq 100 \times \sqrt{\frac{(V_5^2 + V_7^2 + V_{11}^2 + V_{13}^2 + V_{17}^2 + V_{19}^2)}{V_1^2}} \quad (9)$$

produced in the output waveform using the switching angles of Fig. 4 is plotted versus m in Fig. 5

In summary, the polynomial (5) are solved for all possible solutions (sets of switching angles) for any given value of m. The THD produced by the output waveform using each of these sets of switching angles is then computed and the particular solution (set of switching angles) that produces the smallest THD is then chosen. That is, the particular waveform and switching angles are simply dictated by the process of solving the harmonic elimination equations for the solution that produces the lowest THD. Detailed information on the exact intervals of m for which each scheme gives the lowest THD according to Fig. 5 is given in Table I.

VI. Experimental Results

A prototype three-phase 11-level wye-connected cascaded inverter has been built using 100 V, 70 A MOSFETs as the switching devices. The gate driver boards and MOSFETs are shown in Fig. 6. A battery bank of 15 SDCSs each feed the inverter configured with five SDCSs per phase [15]. In the experimental study here, this prototype system was configured to be seven-levels or equivalently, three SDCSs per phase.

The ribbon cable shown in the figure provides the communication link between the gate driver board and the real-time processor. In this work, a real-time computing platform from Opal Technologies [16] was used to interface the computer (which generates the logic signals) to this cable. This system allows one to implement the switching algorithm as a lookup table in Simulink which is then converted to *C* code using RTW (real-time workshop) from *Mathworks*. The RTLab software

$$S_{a,b}(x_1, x_2) \triangleq \begin{bmatrix} a_0(x_1,x_2) & 0 & b_0(x_1,x_2) & 0 & 0 \\ a_1(x_1,x_2) & a_0(x_1,x_2) & b_1(x_1,x_2) & b_0(x_1,x_2) & 0 \\ a_2(x_1,x_2) & a_1(x_1,x_2) & b_2(x_1,x_2) & b_1(x_1,x_2) & b_0(x_1,x_2) \\ a_3(x_1,x_2) & a_2(x_1,x_2) & 0 & b_2(x_1,x_2) & b_1(x_1,x_2) \\ 0 & a_3(x_1,x_2) & 0 & 0 & b_2(x_1,x_2) \end{bmatrix}.$$

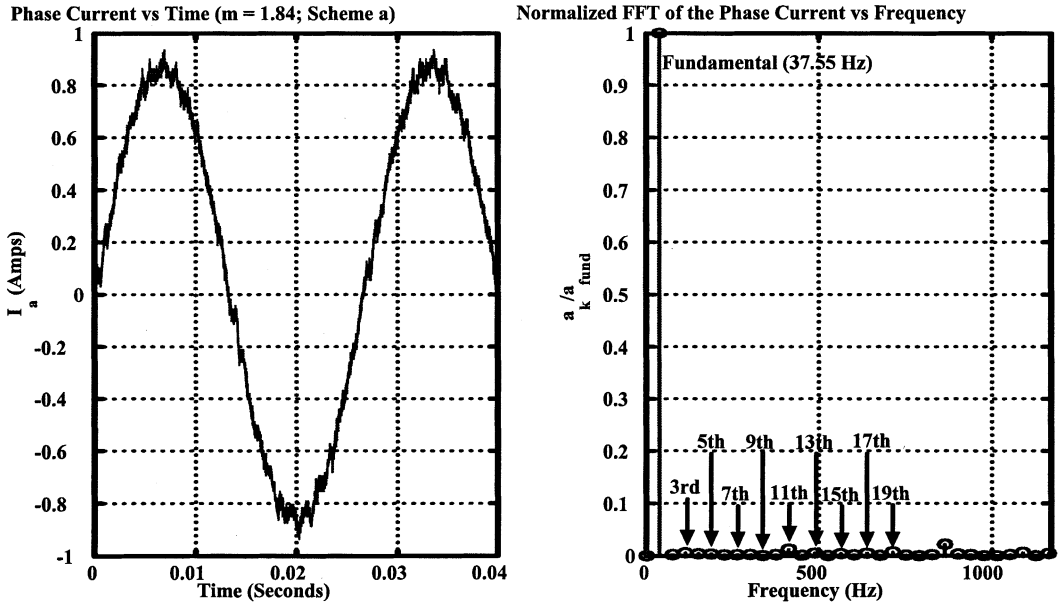

(a) (b)

Fig. 8. (a) Scheme *a* current waveform for $m = 1.84$. (b) Corresponding FFT.

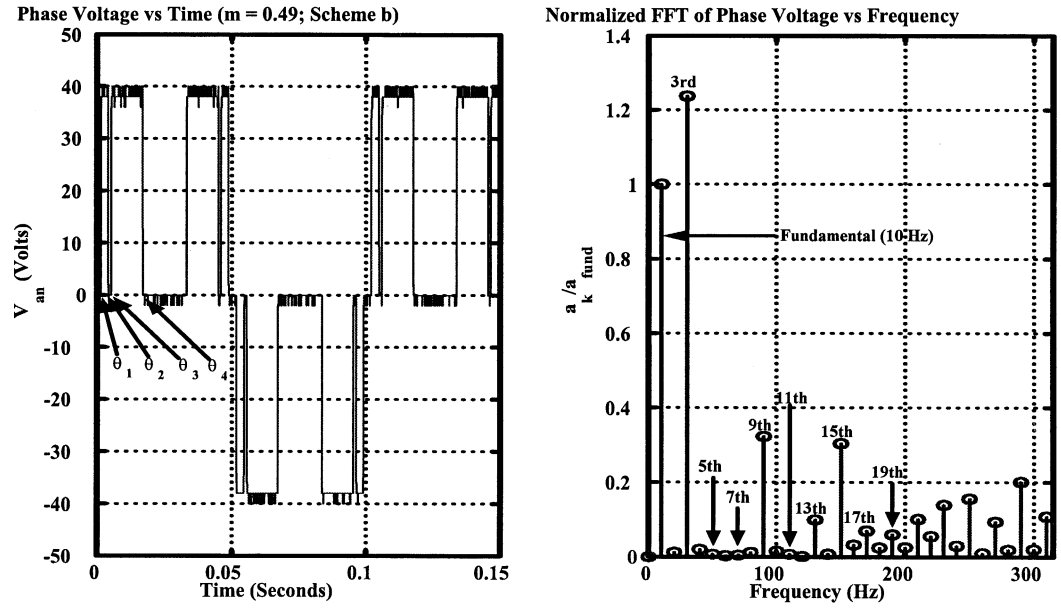

(a) (b)

Fig. 9. (a) Scheme *b* voltage waveform for $m = 0.49$. (b) Corresponding FFT.

[16] provides icons to interface the SIMULINK model to the digital I/O board and converts the *C* code into executables.

The time step size of the control loop was 32 μm or, in other words, the precision error for the time at which a switch is turned on or off was bounded by 32 μm. The real-time implementation is accomplished by placing the data (i.e., Fig. 4) in a lookup table and therefore does not require high computational power for implementation. The voltage level for each separate dc source was nominally charged to 38.6 V. The actual voltages were measured and are given in Table II.

The multilevel converter was attached to a three phase induction motor with the following nameplate data

$$\text{Rated hp} = \frac{1}{3}\ \text{hp}$$

$$\text{Rated Current} = 1.5\ \text{A}$$

$$\text{Rated Speed} = 1725\ \text{rpm}$$

$$\text{Rated Voltage} = 208\ \text{V}\ (\text{RMS line} - \text{to} - \text{line}\ @\ 60\ \text{Hz}).$$

The following set of experiments were chosen to illustrate each of the possible output waveforms. For each such waveform,

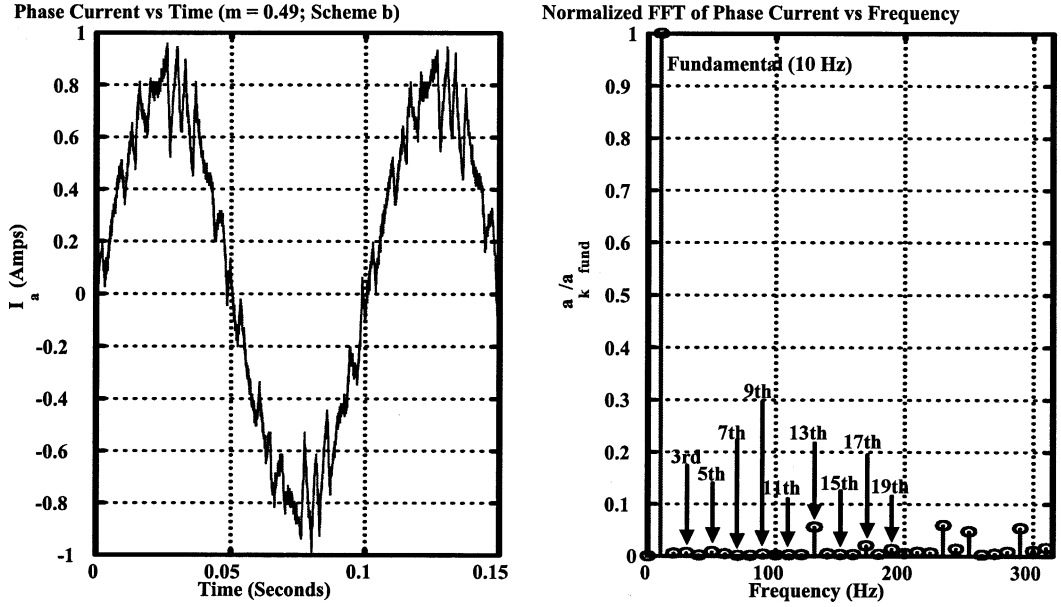

(a) (b)

Fig. 10. (a) Scheme *b* current waveform for $m = 0.49$. (b) Corresponding FFT.

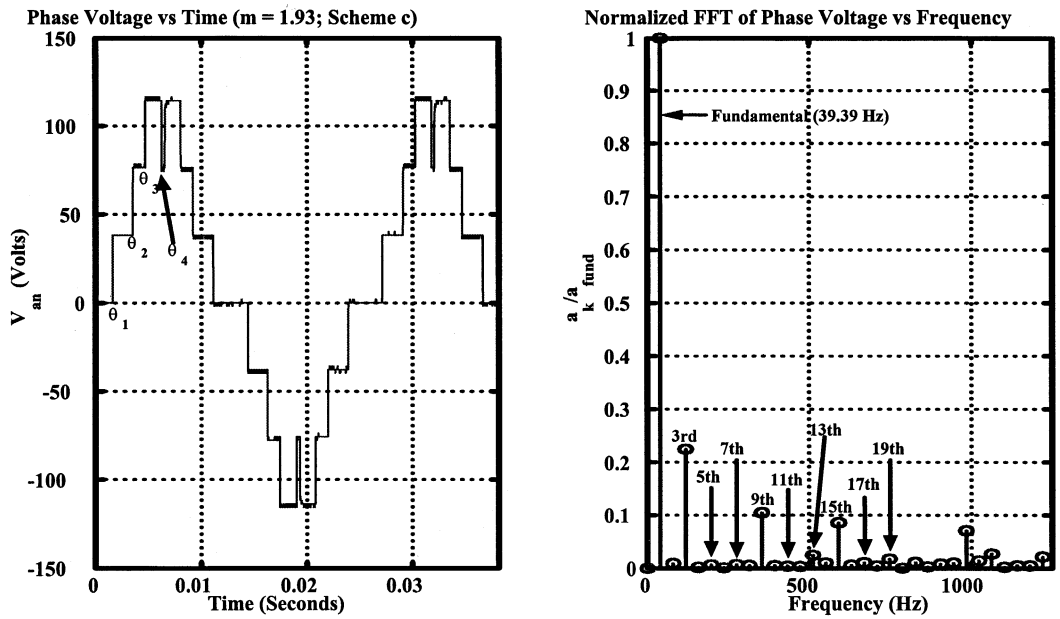

(a) (b)

Fig. 11. (a) Scheme *c* voltage waveform for $m = 1.93$. (b) Corresponding FFT.

a value of m was chosen for which that waveform produced the smallest THD. The phase voltages and currents of the motor were collected and analyzed as given below.

A. Scheme a

For $m = 1.84$, scheme *a* gives the smallest THD. Fig. 7 shows the output waveform for phase *a* and its corresponding FFT with $m = 1.84$. In this case, the fifth and seventh harmonics are zero as expected. Note that the 11th harmonic is not zero, but this is the only scheme in Fig. 3 that does not guarantee the 11th harmonic is zero. The THD in the voltage waveform was computed according to (9) using the FFT data of Fig. 7 giving 3.2%. This corresponds well with the theoretically predicted value of 2.64% given in Fig. 5. The current waveform for phase *a* and its corresponding FFT are given in Fig. 8. The THD in the current was computed and found to be 1.8% which is less than the voltage THD due to filtering by the motor's inductance.

B. Scheme b

Here $m = 0.49$ and scheme *b* (unipolar PWM) produces the smallest THD. Fig. 9 shows the output waveform for phase *a* and its corresponding FFT. In this case, the fifth, seventh, and 11th harmonics are zero as predicted. The THD in the voltage waveform was computed according to (9) using the FFT data

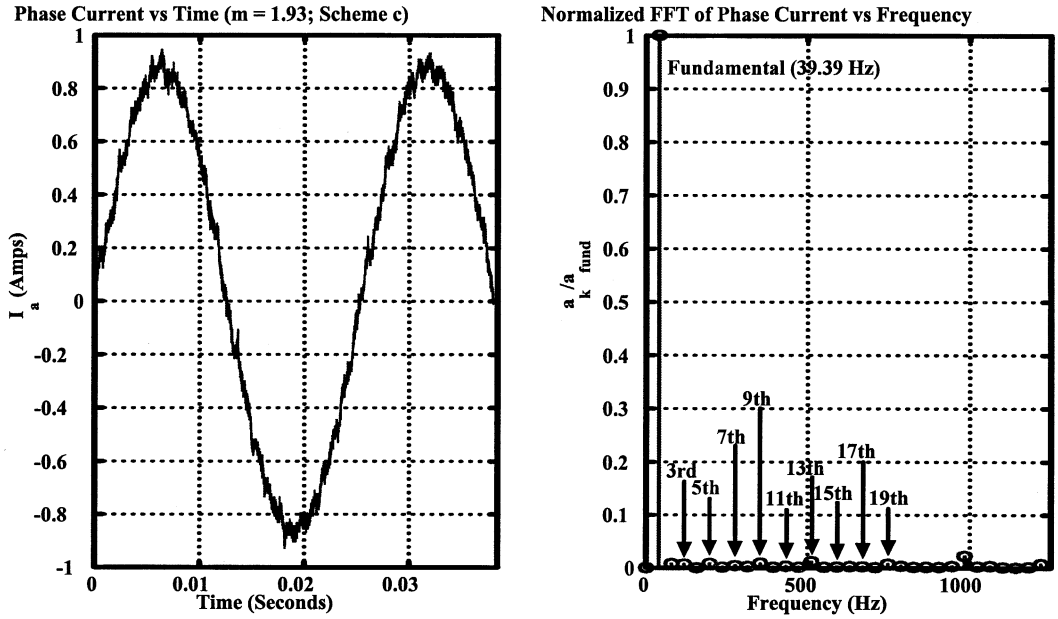

(a) (b)

Fig. 12. (a) Scheme *c* current waveform for $m = 1.93$. (b) Corresponding FFT.

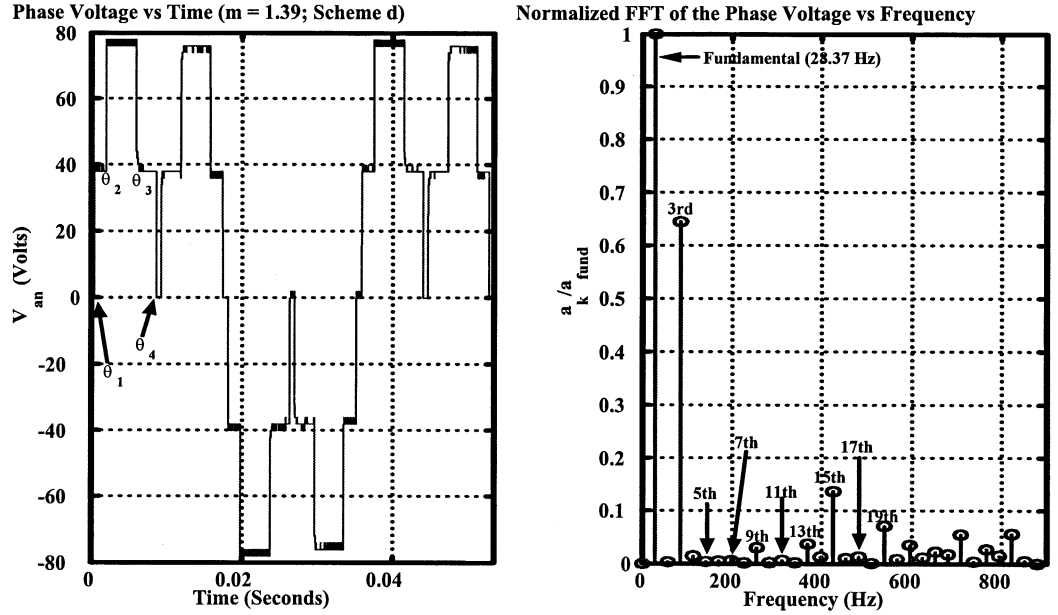

(a) (b)

Fig. 13. (a) Scheme *d* voltage waveform. (b) Corresponding FFT.

of Fig. 9 giving 13.6%. This corresponds well with the theoretically predicted value of 11.4% given in Fig. 5. The current waveform for phase *a* and its corresponding FFT are given in Fig. 10. The THD in the current was computed and found to be 6.2%.

C. Scheme c

For $m = 1.93$, scheme *c* produces the smallest THD. Fig. 11 shows the output waveform for phase *a* and its corresponding FFT. As predicted, the fifth, seventh, and 11th harmonics are all zero. The THD in the voltage waveform was computed according to (9) using the FFT data of Fig. 11 giving 3.37%. This corresponds well with the theoretically predicted value of 2.77% given in Fig. 5. The current waveform for phase *a* and its corresponding FFT are given in Fig. 12. The THD in the current was computed and found to be 2.14%.

D. Scheme d

For $m = 1.39$, scheme *d* produces the smallest THD. Fig. 13 shows the output waveform for phase *a* and its corresponding

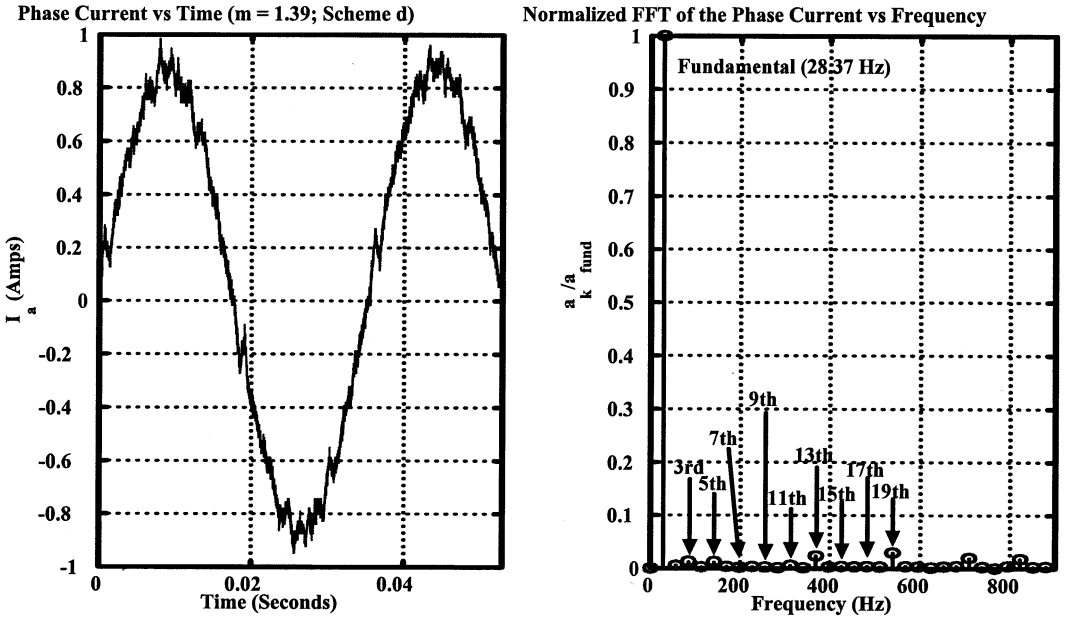

(a) (b)

Fig. 14. (a) Scheme *d* current waveform for $m = 1.39$. (b) Corresponding FFT.

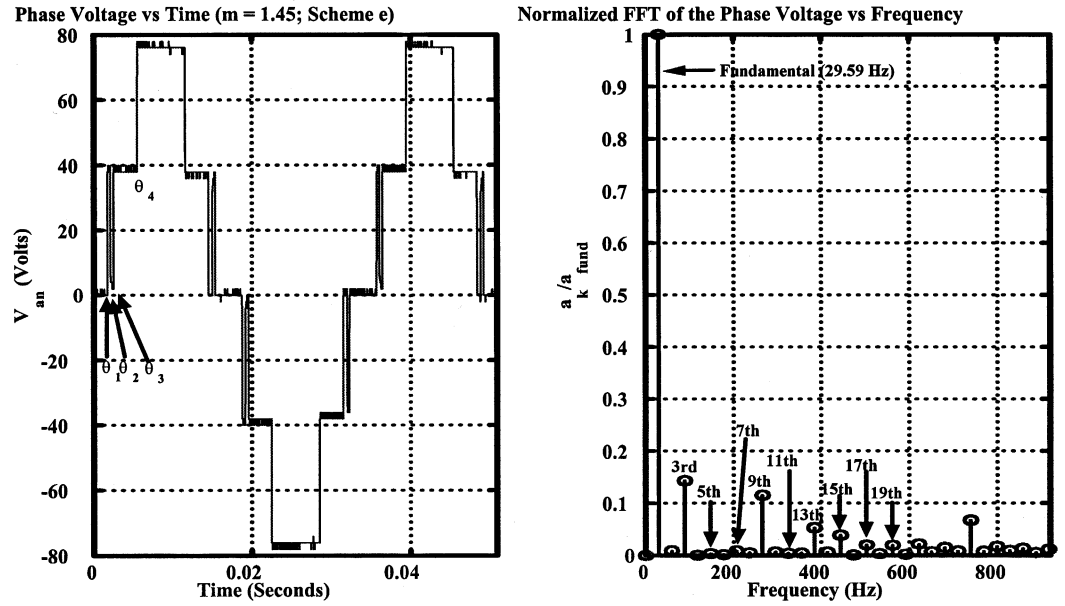

(a) (b)

Fig. 15. (a) Scheme *e* voltage waveform for $m = 1.45$. (b) Corresponding FFT.

FFT. As predicted, the fifth, seventh, and 11th harmonics are all zero. The THD in the voltage waveform was computed according to (9) using the FFT data of Fig. 13 giving 8.17%. This corresponds well with the theoretically predicted value of 7% given in Fig. 5. The current waveform for phase *a* and its corresponding FFT are given in Fig. 14. The THD in the current was computed and found to be 4.3%.

E. Scheme e

For $m = 1.45$, scheme *e* produces the smallest THD. Fig. 15 shows the output waveform for phase *a* and its corresponding FFT. Again, as predicted, the fifth, seventh, and 11th harmonics are all zero. The THD in the voltage waveform was computed according to (9) using the FFT data of Fig. 15 giving 6.1%. This corresponds well with the theoretically predicted value of 5.75% given in Fig. 5. The current waveform for phase *a* and its corresponding FFT are given in Fig. 16. The THD in the current was computed and found to be 3.6%.

F. Scheme f

For $m = 1.67$, scheme *f* produces the smallest THD. Fig. 17 shows the output waveform for phase *a* and its corresponding

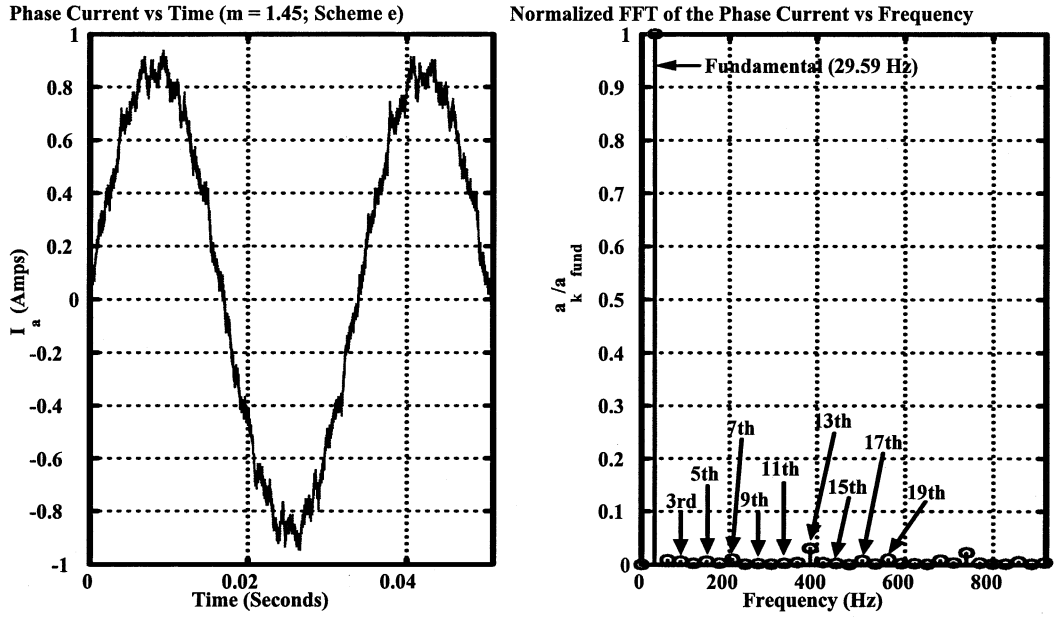

(a) (b)

Fig. 16. (a) Scheme *e* current waveform for $m = 1.45$. (b) Corresponding FFT.

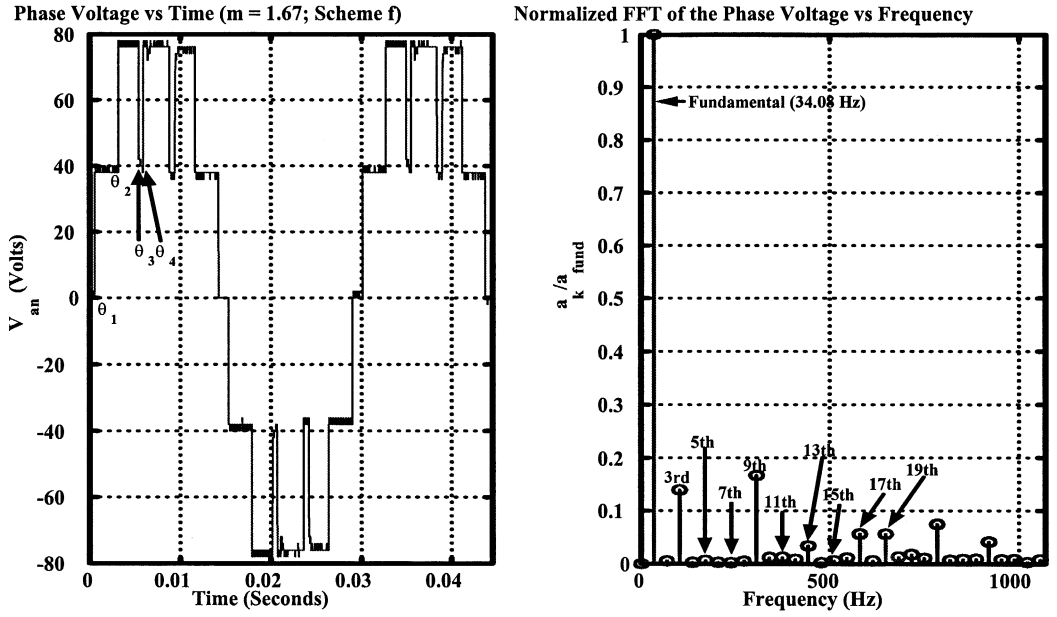

(a) (b)

Fig. 17. (a) Scheme *f* voltage waveform for $m = 1.67$. (b) Corresponding FFT.

FFT. Again, as predicted, the fifth, seventh, and 11th harmonics are all zero. The THD in the voltage waveform was computed according to (9) using the FFT data of Fig. 17 giving 8.73%. This corresponds well with the theoretically predicted value of 8.9% given in Fig. 5. The current waveform for phase a and its corresponding FFT are given in Fig. 18. The THD in the current was computed and found to be 4.8%.

VII. Conclusion

A unified procedure to eliminate harmonics in a multilevel inverter has been presented along with experimental verification. The methodology transforms the sets of transcendental harmonic elimination equations for all of the possible output waveforms into a single set of polynomial equations. For each value of $m(m_a = m/s)$, the complete set of solutions to these polynomial equations are found using resultant theory. The particular solution chosen is that one which results in the smallest value of the THD computed according to (9). The output waveform is simply dictated by the particular set of switching angles computed for that value of m which give the smallest THD. This procedure results in a lookup table that gives the switching angles as a function the parameter m. Experimental results were in agreement with the predicted results.

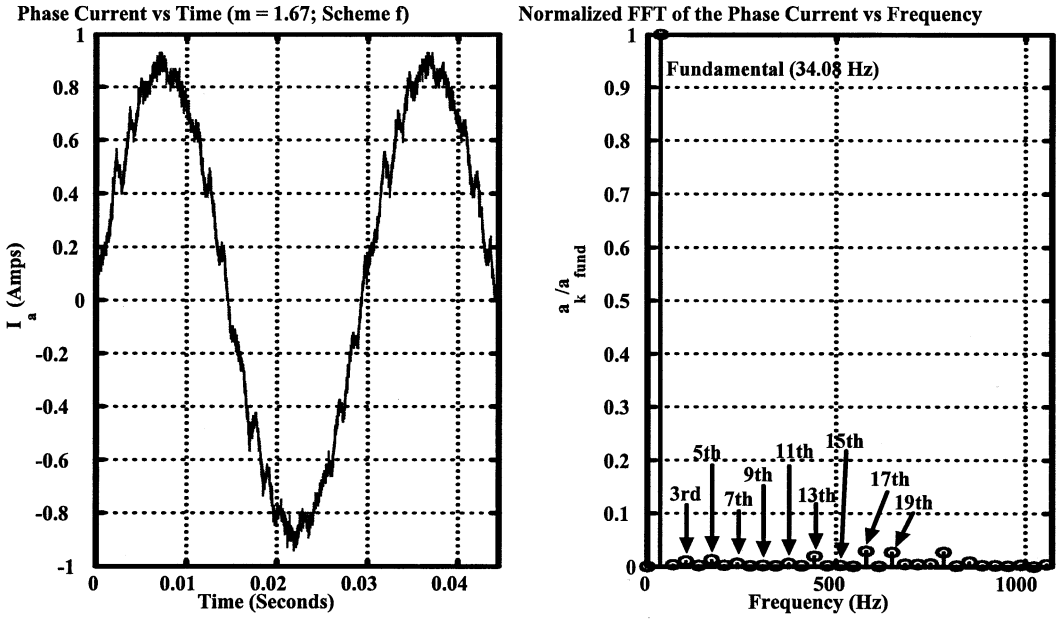

(a) (b)

Fig. 18. (a) Scheme *f* current waveform for $m = 1.67$. (b) Corresponding FFT.

APPENDIX

RESULTANTS

Given two polynomials $a(x_1, x_2)$ and $b(x_1, x_2)$ how does one find their common zeros? That is, the values (x_{10}, x_{20}) such that

$$a(x_{10}, x_{20}) = b(x_{10}, x_{20}) = 0.$$

Consider $a(x_1, x_2)$ and $b(x_1, x_2)$ as polynomials in x_2 whose coefficients are polynomials in x_1. For example, let $a(x_1, x_2)$ and $b(x_1, x_2)$ have degrees 3 and 2, respectively in x_2 so that they may be written in the form

$$\begin{aligned} a(x_1, x_2) &= a_3(x_1)x_2^3 + a_2(x_1)x_2^2 + a_1(x_1)x_2 + a_0(x_1) \\ b(x_1, x_2) &= b_2(x_1)x_2^2 + b_1(x_1)x_2 + b_0(x_1). \end{aligned}$$

In general, there is always a polynomial $r(x_1)$ (called the *resultant polynomial*) such that

$$\alpha(x_1, x_2)a(x_1, x_2) + \beta(x_1, x_2)b(x_1, x_2) = r(x_1).$$

So if $a(x_{10}, x_{20}) = b(x_{10}, x_{20}) = 0$ then $r(x_{10}) = 0$, that is, if (x_{10}, x_{20}) is a common zero of the pair $\{a(x_1, x_2), b(x_1, x_2)\}$, then the first coordinate x_{10} is a zero of $r(x_1) = 0$. The roots of $r(x_1)$ are easy to find (numerically) as it is a polynomial in one variable. To find the common zeros of $\{a(x_1, x_2), b(x_1, x_2)\}$, one computes all roots x_{1i} $i = 1, \ldots n_1$ of $r(x_1)$. Next, for each such x_{1i}, one (numerically) computes the roots of

$$a(x_1, x_2) = 0 \tag{10}$$

and the roots of

$$b(x_1, x_2) = 0. \tag{11}$$

Any root x_{2j} that is in the solution set of both (10) and (11) for a given x_{1i} results in the pair (x_{1i}, x_{2j}) being a common zero of $a(x_1, x_2)$ and $b(x_1, x_2)$. Thus, this gives a method of solving polynomials in one variable to compute all of the common zeros of $\{a(x_1, x_2), b(x_1, x_2)\}$.

To see how one obtains $r(x_1)$, let

$$\begin{aligned} a(x_1, x_2) &= a_3(x_1)x_2^3 + a_2(x_1)x_2^2 + a_1(x_1)x_2 + a_0(x_1) \\ b(x_1, x_2) &= b_2(x_1)x_2^2 + b_1(x_1)x_2 + b_0(x_1). \end{aligned}$$

Next, see if polynomials of the form

$$\begin{aligned} \alpha(x_1, x_2) &= \alpha_1(x_1)x_2 + \alpha_0(x_1) \\ \beta(x_1, x_2) &= \beta_2(x_1)x_2^2 + \beta_1(x_1)x_2 + \beta_0(x_1) \end{aligned}$$

can be found such that

$$\alpha(x_1, x_2)a(x_1, x_2) + \beta(x_1, x_2)b(x_1, x_2) = r(x_1). \tag{12}$$

Equating powers of x_2, this equation may be rewritten in matrix form as

$$\begin{bmatrix} a_0 & 0 & b_0 & 0 & 0 \\ a_1 & a_0 & b_1 & b_0 & 0 \\ a_2 & a_1 & b_2 & b_1 & b_0 \\ a_3 & a_2 & 0 & b_2 & b_1 \\ 0 & a_3 & 0 & 0 & b_2 \end{bmatrix} \begin{bmatrix} \alpha_0(x_1) \\ \alpha_1(x_1) \\ \beta_0(x_1) \\ \beta_1(x_1) \\ \beta_2(x_1) \end{bmatrix} = \begin{bmatrix} r(x_1) \\ 0 \\ 0 \\ 0 \\ 0 \end{bmatrix}.$$

The matrix on the left-hand side is called the *Sylvester* matrix and is denoted here by $S_{a,b}(x_1)$. The inverse of $S_{a,b}(x_1)$ has the form

$$S_{a,b}^{-1}(x_1) = \frac{1}{\det S_{a,b}(x_1)} \operatorname{adj}(S_{a,b}(x_1))$$

where $\mathrm{adj}(S_{a,b}(x_1))$ is the adjoint matrix and is a 5×5 *polynomial* matrix in x_1. Solving for $\alpha_i(x_1)$, $\beta_i(x_1)$ gives

$$\begin{bmatrix} \alpha_0(x_1) \\ \alpha_1(x_1) \\ \beta_0(x_1) \\ \beta_1(x_1) \\ \beta_2(x_1) \end{bmatrix} = \frac{\mathrm{adj}\ S_{a,b}(x_1)}{\det S_{a,b}(x_1)} \begin{bmatrix} r(x_1) \\ 0 \\ 0 \\ 0 \\ 0 \end{bmatrix}.$$

Choosing $r(x_1) = \det S_{a,b}(x_1)$ this becomes

$$\begin{bmatrix} \alpha_0(x_1) \\ \alpha_1(x_1) \\ \beta_0(x_1) \\ \beta_1(x_1) \\ \beta_2(x_1) \end{bmatrix} = \mathrm{adj}\ S_{a,b}(x_1) \begin{bmatrix} 1 \\ 0 \\ 0 \\ 0 \\ 0 \end{bmatrix}$$

and guarantees that $\alpha_0(x_1), \alpha_1(x_1), \beta_0(x_1), \beta_1(x_1), \beta_2(x_1)$ are *polynomials* in x_1. That is, the *resultant polynomial* defined by $r(x_1) = \det S_{a,b}(x_1)$ is the polynomial required for (12).

REFERENCES

[1] L. M. Tolbert and F. Z. Peng, "Multilevel converters as a utility interface for renewable energy systems," in *Proc. IEEE Power Eng. Soc. Summer Meeting*, Seattle, WA, July 2000, pp. 1271–1274.

[2] L. M. Tolbert, F. Z. Peng, and T. G. Habetler, "Multilevel converters for large electric drives," *IEEE Trans. Ind. Applicat.*, vol. 35, pp. 36–44, Jan./Feb. 1999.

[3] J. S. Lai and F. Z. Peng, "Multilevel converters—a new breed of power converters," *IEEE Trans. Ind. Applicat.*, vol. 32, pp. 509–517, May/June 1996.

[4] J. Chiasson, L. M. Tolbert, K. McKenzie, and Z. Du, "Eliminating harmonics in a multilevel inverter using resultant theory," in *Proc. IEEE Power Electron. Spec. Conf.*, Cairns, Australia, June 2002, pp. 503–508.

[5] ——, "A complete solution to the harmonic elimination problem," in *Proc. Appl. Power Electron. Conf. APEC 2003*, Miami, FL, Feb. 2003, pp. 596–602.

[6] F.-S. Shyu and Y.-S. Lai, "Virtual stage pulse-width modulation technique for multilevel inverter/converter," *IEEE Trans. Power Electron.*, vol. 17, pp. 332–341, May 2002.

[7] L. M. Tolbert, F. Z. Peng, and T. G. Habetler, "Multilevel PWM methods at low modulation indexes," *IEEE Trans. Power Electron.*, vol. 15, pp. 719–725, July 2000.

[8] D. Cox, J. Little, and D. O'Shea, *Ideals, Varieties, and Algorithms: An Introduction to Computational Algebraic Geometry and Commutative Algebra*, 2nd ed. New York: Springer-Verlag, 1996.

[9] P. N. Enjeti, P. D. Ziogas, and J. F. Lindsay, "Programmed PWM techniques to eliminate harmonics: a critical evaluation," *IEEE Trans. Ind. Applicat.*, vol. 26, pp. 302–316, Mar./Apr. 1990.

[10] H. S. Patel and R. G. Hoft, "Generalized harmonic elimination and voltage control in thryristor inverters: part I—harmonic elimination," *IEEE Trans. Ind. Applicat.*, vol. 9, pp. 310–317, May/June 1973.

[11] ——, "Generalized harmonic elimination and voltage control in thryristor inverters: part II—voltage control technique," *IEEE Trans. Ind. Applicat.*, vol. 10, pp. 666–673, Sept./Oct. 1974.

[12] T. Cunningham, "Cascade multilevel inverters for large hybrid-electric vehicle applications with variant dc sources," M.S. thesis, Univ. Tennessee, Knoxville, 2001.

[13] J. von zur Gathen and J. Gerhard, *Modern Computer Algebra*. Cambridge, U.K.: Cambridge Univ. Press, 1999.

[14] J. Sun and I. Grotstollen, "Pulsewidth modulation based on real-time solution of algebraic harmonic elimination equations," in *Proc. 20th Int. Conf. Ind. Electron., Contr. Instrum. IECON*, vol. 1, 1994, pp. 79–84.

[15] L. M. Tolbert, F. Z. Peng, T. Cunningham, and J. Chiasson, "Charge balance control schemes for cascade multilevel converter in hybrid electric vehicles," *IEEE Trans. Ind. Electron.*, vol. 49, pp. 1058–1064, Oct. 2002.

[16] RTLab, Opal-RT Technologies. (2001). *http://www.opal_rt.com/* [Online]

John N. Chiasson (S'82–M'84–SM'03) received the B.S. degree in mathematics from the University of Arizona, Tucson, the M.S. degree in electrical engineering from Washington State University, Pullman, and the Ph.D. degree in controls from the University of Minnesota, Minneapolis.

He has been with Boeing Aerospace, Control Data, and ABB Daimler-Benz Transportation. Since 1999, he has been on the faculty of Electrical and Computer Engineering, University of Tennessee, where his interests include the control of ac drives, multilevel converters, and hybrid electric vehicles.

Leon M. Tolbert (S'89–M'91–SM'98) received the B.E.E., M.S., and Ph.D. degrees from the Georgia Institute of Technology, Atlanta, all in electrical engineering.

He joined the Engineering Division, Lockheed Martin Energy Systems, in 1991 and worked on several electrical distribution projects at the three U.S. Department of Energy plants in Oak Ridge, TN. In 1997, he became a Research Engineer in the Power Electronics and Electric Machinery Research Center, Oak Ridge National Laboratory (ORNL). In 1999, he was appointed as an Assistant Professor in the Department of Electrical and Computer Engineering, University of Tennessee, Knoxville. He is an Adjunct Participant at ORNL and conducts joint research at the National Transportation Research Center (NTRC). He does research in the areas of electric power conversion for distributed energy sources, motor drives, multilevel converters, hybrid electric vehicles, and application of SiC power electronics.

Dr. Tolbert received the National Science Foundation CAREER Award and the 2001 IEEE Industry Applications Society Outstanding Young Member Award. He is an Associate Editor of the IEEE POWER ELECTRONICS LETTERS and a registered Professional Engineer in the state of Tennessee.

Keith J. McKenzie (S'01) received the B.S. degree in electrical engineering from The University of Tennessee, Knoxville, in 2001 where he is currently pursuing the M.S. degree.

Zhong Du (S'01) received the B.E. and M.E. degrees from Tsinghua University, Bejing, China, in 1996 and 1999, respectively, and is currently pursuing the Ph.D. degree in electrical and computer engineering at The University of Tennessee, Knoxville.

He has worked in the area of computer networks, both in academia as well as in industry. His research interests include power electronics and computer networks.